Observation of a dynamical mixing process of exciton-polaritons in a ZnSe epitaxial layer using four-wave mixing spectroscopy

H. Tahara,[1] M. Bamba,[2] Y. Ogawa,[1] and F. Minami[1]

[1]*Department of Physics, Tokyo Institute of Technology, Oh-Okayama 2-12-1, Tokyo 152-8551, Japan*

[2]*Laboratoire Matériaux et Phénomènes Quantiques, Université Paris Diderot-Paris 7 et CNRS, Bâtiment Condorcet, 10 rue Alice Domon et Léonie Duquet, 75205 Paris Cedex 13, France*

(Received 11 March 2012; revised manuscript received 21 August 2012; published 26 December 2012)

We have observed a coherent spectral change of exciton-polaritons in a ZnSe epitaxial layer through spectrally resolved four-wave mixing spectroscopy. The spectra exhibit an exchange of the dominant peak position between the different polariton branches depending on the delay time of the second pulse. This result reflects the initial creation process of polaritons with many-body interactions. The calculation based on the exciton-photon microscopic model reveals that the spectral change occurs due to the four-particle correlations between heavy-hole and light-hole excitons; it clearly shows the dynamical mixing process of exciton-polaritons in the initial creation.

DOI: 10.1103/PhysRevB.86.235208 PACS number(s): 71.36.+c, 78.66.Hf, 78.47.nj, 42.50.Md

I. INTRODUCTION

An exciton-polariton is a quasiparticle consisting of an exciton and a photon, and it is the eigenstate of electromagnetic fields in semiconductors around the exciton resonance. The propagation of exciton-polaritons in semiconductors has been investigated by the time-resolved measurements of a transmitted pulse in which polariton beats have been observed.[1–3] In contrast to these studies of the propagation process, the initial creation process of polaritons has not been sufficiently investigated. In the initial creation process, the periodic changes of quantum state between excitons and photons, i.e., the Rabi oscillations, are expected to be observed as the interference between different polariton branches. This fundamental phenomenon of exciton-polaritons, however, is complicated by the dephasing and nonlinear processes; the transient dynamics of the exciton-photon system in the process still remain unclear. The weak signal of the creation process cannot be distinguished from the strong signal of the propagating pulse in transmission measurements.

For the observation of the dynamics in coherent processes, four-wave mixing (FWM) is the most suitable technique. The influence of the exciton-exciton interaction on exciton dephasing has been investigated both experimentally and theoretically.[4–10] These studies have revealed the effects depending on excitation density, which are described as excitation-induced dephasing, excitation-induced shift, local-field effects, and biexciton formation. Furthermore, in the spectral domain, biexciton contribution and two-pair correlations have been reported in the studies at negative delay times of FWM measurements.[11–14]

In this paper, we report the coherent spectral changes of exciton-polaritons in a ZnSe epitaxial layer. Using the spectrally resolved (SR) FWM technique, we have successfully observed the characteristic spectra clearly reflecting the initial creation process. For usual quantum beats in the system of bare excitons, such as the system including heavy-hole and light-hole excitons, the relative phase between two states is independent of the delay time in the FWM spectra. In contrast, the observed FWM spectra in our experiment are dramatically changed with time due to the dynamical mixing of exciton-polaritons.

II. EXPERIMENTAL DETAILS

The investigated ZnSe epitaxial layer was grown on a GaAs(001) substrate by metalorganic chemical vapor deposition (MOCVD). The epitaxial layer with a thickness of 4.7 μm is under biaxial tensile strain due to the lattice mismatch and the difference in thermal expansion between the ZnSe layer and the GaAs substrate.[15,16] The strain splits the valence band into the heavy-hole (hh) and light-hole (lh) bands. The exciton-polaritons show three-branch dispersion due to the mixing of the photon, hh, and lh excitons, which have been investigated using resonant Brillouin scattering.[17,18] For excitation pulses, we used a frequency-doubled mode-locked Ti:sapphire laser with a central energy of 2.802 eV, whose duration and repetition rate were 100 fs and 76 MHz, respectively. Four-wave mixing (FWM) measurements were performed in reflection geometry using two excitation pulses with right circular polarization. The first (second) excitation pulse was incident on the sample with a wave vector $\boldsymbol{k}_1$ ($\boldsymbol{k}_2$). The FWM signal in the direction of $2\boldsymbol{k}_2-\boldsymbol{k}_1$ was spectrally resolved by a monochromator and detected by a photomultiplier tube. The sample was measured at 3.5 K in a closed-cycle refrigerator.

The polariton dispersion is calculated for the ZnSe epitaxial layer as shown in Fig. 1(a). The details for calculated dispersion curves are explained in the Appendix. In the calculation, the energy splitting between the hh and lh excitons due to biaxial strain is set at 2.1 meV, and this value is consistent with those reported in previous investigations.[15,16,18] The filled spectrum in Fig. 1(a) shows the FWM signal measured at the delay time of 4.4 ps. Taking into account the polariton dispersion, the peak positions are determined by the following two competitive factors: (i) strong optical coupling realized near the light line in the dispersion and (ii) the high density of states (DOS) realized on the excitonlike dispersion. Actually the peaks in the spectrum, which are indicated as dashed lines, correspond well to the points on the dispersion, satisfying both conditions. The lower, middle, and upper polariton (LP, MP, and UP) peaks are observed at 2801.4, 2803.0, and 2805.9 meV, respectively. The UP peak is relatively small in the three peaks due to the above factors. The corresponding wave

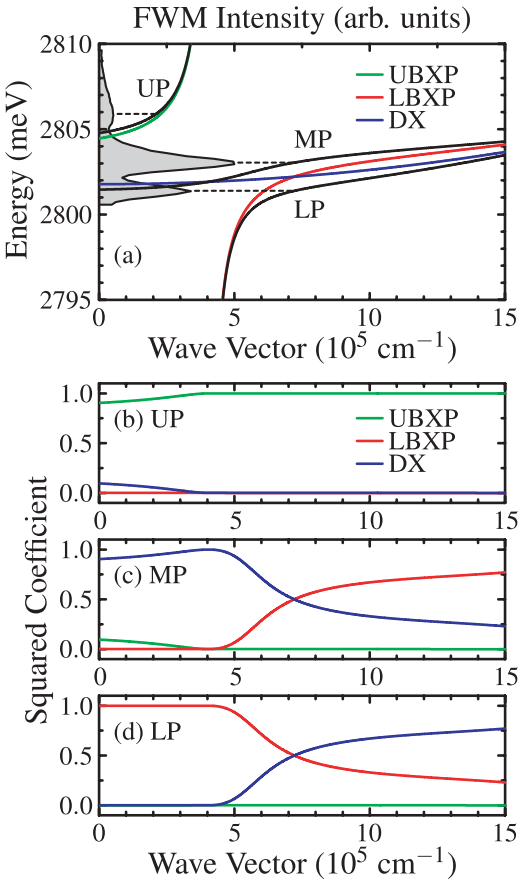

FIG. 1. (Color online) (a) Calculated dispersions of a three-branch polariton (black solid lines), upper bright exciton-polariton (UBXP) (green solid line), lower bright exciton-polariton (LBXP) (red solid line), and dark exciton (DX) (blue solid line) in the ZnSe epitaxial layer. The FWM signal (filled spectrum) was experimentally measured at the delay time of 4.4 ps. Dashed lines indicate the peaks of the spectrum. Squared coefficients are calculated for UBXP, LBXP, and DX in (b) upper, (c) middle, and (d) lower polaritons (UP, MP, and LP).

vectors of the LP and MP are equal to each other at 7.2×10^5 cm^{-1}, whereas that of the UP is 2.1×10^5 cm^{-1}.

For analyzing the peaks accurately, three-branch polaritons are redescribed by the bases including the bright exciton (BX) and dark exciton (DX), instead of those of the photon, hh, and lh excitons.[17,19] As a linear combination of hh and lh excitons, the BX and DX can be represented in terms of the total angular momentum $\boldsymbol{J}$. The BX (DX) is defined as the state with $J = 1$ and $J_z = \pm 1$ ($J = 2$ and $J_z = \pm 1$). The optically allowed BX is coupled with a photon, thereby generating upper and lower bright exciton-polaritons (UBXP and LBXP); in contrast, the DX is optically forbidden. The DX contributes the polariton branches through the coupling with the UBXP or LBXP, which depends on the strain splitting between the hh and lh bands. The UBXP, LBXP, and DX branches are shown in Fig. 1(a). The components (squared coefficients) of the UBXP, LBXP, and DX in the three-branch polariton are shown in Figs. 1(b)–1(d). The UP branch is quite similar to the UBXP branch [see Fig. 1(b)], and there is little contribution of the UBXP in the LP and MP branches [see Figs. 1(c) and 1(d)]. The coefficient of the LBXP coincides with that of the DX at the wave vector of 7.2×10^5 cm^{-1}, at which the LP and MP peaks are observed in the FWM spectrum, as shown in Fig. 1(a). Taking into account these coefficients, the two dominant peaks (LP and MP) in the FWM spectra are described by the dynamics of the LBXP and DX, and the contribution of the UBXP for the two peaks is negligible.

III. RESULTS AND DISCUSSION

In order to observe the dynamical mixing between the LP and MP, the SR-FWM measurement was performed by changing the delay time from 0.0 to 4.8 ps; the measurement results are shown in Fig. 2(a). In the delay time range from 0.0 to 2.0 ps, the spectra exhibit a single peak, which appears as a fast-decay component in the FWM measurements, instead of the two peaks of the LP and MP. This single peak is the fast-decay signal due to the LBXP at a stage prior to the mixing process of the LBXP and DX. In reflection geometry, FWM signals are generated in the near-surface region; the fast-decay component is the signal generated by the propagating pulse of the LBXP in this region. It arises only for short delay times, because the propagating pulse of the first excitation cannot remain in the region for long delay times, i.e., it is absorbed inside the sample. As seen in Fig. 2(a), the mixing process gradually becomes pronounced after a delay time of 2.0 ps. The two peaks at -0.8 and 0.8 meV correspond to the LP and MP peaks, respectively. These two peaks originate from the exciton-polaritons remaining in the near-surface region as mixed states of the LBXP and DX. The spectra exhibit an exchange of the dominant peak position between the two peaks as shown in the figure. The MP peak is dominant at delay times of 2.0 and 2.4 ps. In contrast, the LP becomes dominant as a substitute for the MP at delay times of 2.8 and 3.2 ps.

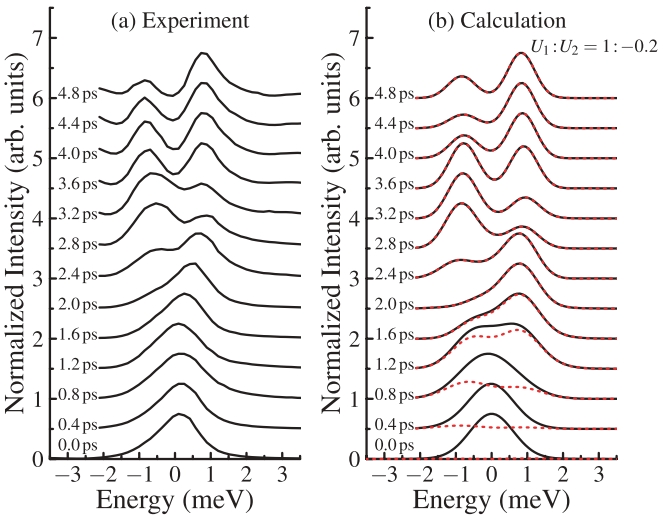

FIG. 2. (Color online) (a) Experimental and (b) theoretical spectrally resolved FWM signal for delay times from 0.0 to 4.8 ps in 0.4-ps steps as indicated. The energy of 2802.2 meV is set to the zero of the energy axis as the energy reference. The calculation is performed with $U_1 : U_2 = 1 : -0.2$. The signal indicated by the dotted line is calculated without the fast-decay component. The spectra are normalized for each delay time.

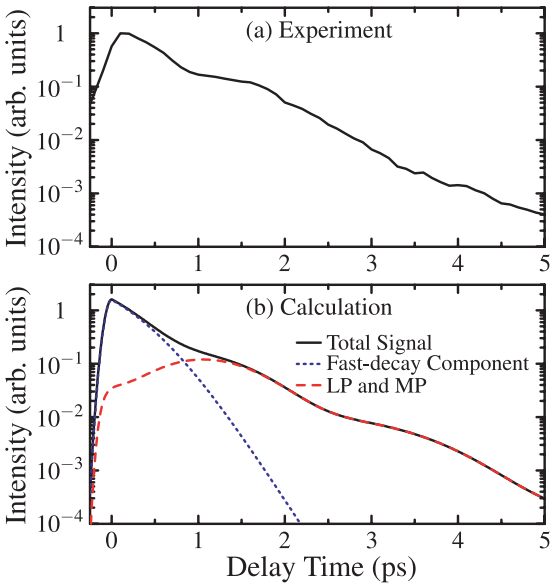

FIG. 3. (Color online) (a) Experimental and (b) theoretical time-integrated FWM signal as a function of delay time. The calculation includes the fast-decay component (dotted line), LP and MP (dashed line), and total signal (solid line) conditions.

Subsequently, the MP grows dominant again. The exchange behavior is independent of the excitation intensity; it exhibits the third-order nonlinear response of FWM signals.

This spectral change shows the initial creation process of the LP and MP, and it is reproduced by the calculation shown in Fig. 2(b), which is explained later in detail. The exchange behavior is not observed in bare exciton systems, including quantum-beat phenomena. In a quantum-beat system including hh and lh excitons, the intensity ratio between the hh and lh exciton peaks in FWM spectra is independent of delay times; however, these excitons exhibit intensity oscillation, i.e., quantum beats, in time-integrated (TI) FWM measurements for each peaks.[20,21] In contrast, the observed spectra in our experiment strongly depend on delay times, although the TI-FWM signal does not exhibit a beat structure as shown in Fig. 3(a) . The spectral change is a characteristic feature in the initial process of exciton-polaritons. The LBXP is firstly driven in the near-surface region, and then the DX is gradually excited through the coupling between these states. The exchange of the dominant peak position in the FWM spectra reflects the complicated nonlinear interactions between the LBXP and DX, as we discuss below.

In order to understand theoretically the spectral change, we take into account the microscopic four-particle interaction between the LBXP and DX as the exciton-exciton interaction. We focus only on the LBXP and DX around the wave vector of 7.2×10^5 cm^{-1}, and their energies are assumed to be equal to $\hbar\omega_0$ for simplicity. The total Hamiltonian in the material is expressed as $H_{\rm m} = H_0 + H_1$, with

$$H_0 = \sum_k (\hbar\omega_0 p_k^\dagger p_k + \hbar\omega_0 d_k^\dagger d_k + iCp_k^\dagger d_k - iCd_k^\dagger p_k), \quad (1)$$

$$H_1 = U_1\left(h_{2k_2-k_1}^\dagger h_{k_1}^\dagger h_{k_2} h_{k_2} + l_{2k_2-k_1}^\dagger l_{k_1}^\dagger l_{k_2} l_{k_2}\right) + 2U_2\left(h_{2k_2-k_1}^\dagger l_{k_1}^\dagger h_{k_2} l_{k_2} + l_{2k_2-k_1}^\dagger h_{k_1}^\dagger h_{k_2} l_{k_2}\right), \quad (2)$$

where p_k and d_k denote the annihilation operators for the LBXP and DX with the wave vector k, respectively; C denotes the coupling constant between the LBXP and DX. The eigenenergy of LP (MP) corresponds to $\hbar\omega_0 - C$ ($\hbar\omega_0 + C$). In the ZnSe epitaxial layer, the hh and lh excitons interact with each other via three types of exciton-exciton interactions, i.e., the interactions of hh-hh, hh-lh, and lh-lh excitons. The nonlinear interaction Hamiltonian H_1 includes all the exciton-exciton interactions for hh and lh exciton systems, which is investigated as the weakly interacting boson model in semiconductors.[22,23] Here, h_k and l_k denote the annihilation operators for the hh and lh excitons and they are defined as $h_k = -i(\sqrt{3}/2)p_k + (1/2)d_k$ and $l_k = i(1/2)p_k + (\sqrt{3}/2)d_k$, respectively. The strength of the hh-hh exciton interaction U_1 is assumed to be identical to that of the lh-lh exciton interaction; the strength of the hh-lh exciton interaction U_2 is expressed as a different value. The four-particle correlations of hh and lh excitons in H_1 exhibit complicated interactions between the LBXP and DX, and these interactions cause the change of the spectral shape depending on the delay time. In the nonlinear interaction Hamiltonian, we pick up the terms including the creation operator with the wave vector $2k_2 - k_1$, because the FWM signals in the direction of $2\boldsymbol{k}_2 - \boldsymbol{k}_1$ were measured.

With regard to the expression of the excitation pulses, we consider that the LBXP is driven by input light pulses as follows: $H_2 = \sum_{j=1,2} i\hbar A_j \exp[-i\omega_0(t - t_j)] \exp[-(t - t_j)^2/\tau_{\rm p}^2] p_{k_j}^\dagger + {\rm H.c.}$, where A_1 (A_2) and t_1 (t_2) denote the excitation amplitude and the excitation time for the first (second) pulse, respectively; $\tau_{\rm p}$ indicates the pulse duration. The second term is the Hermitian conjugate (H.c.) of the first term. Excitation pulses generate only optically allowed LBXP because the DX is optically forbidden. The LBXP is firstly driven in the near-surface region, and then the DX is gradually excited through the coupling between these states. The pulse energy is set at the resonant energy of LBXP, i.e., $\hbar\omega_0$.

The Heisenberg equation of motion for p_k and d_k has been calculated up to the third order in powers of H_2, where we assume that the nonlinear interactions are sufficiently weak for the higher-order terms to be neglected in FWM signals. The decay of LBXP and DX is effectively introduced by replacing ω_0 with $\omega_0 - i\Gamma$ in Eq. (1), where Γ is the decay constant. It should be noted that the FWM signal in reflection geometry is generated in the near-surface region, and that the decay constant includes both dephasing and escape of propagating polaritons from the region. Since the sample exhibits an inhomogeneous broadening of resonances of the LBXP and DX, the FWM signal is emitted as a photon echo. The FWM signal with the inhomogeneous broadening $P_{\rm i}(t)$ is expressed as $P_{\rm i}(t) = \int_{-\infty}^{\infty} d\omega_0 g(\omega_0) p_{2k_2-k_1}(t)$, where $g(\omega_0)$ is the inhomogeneous broadening function assumed as a Gaussian ensemble.[24] The amplitude of the optically forbidden DX is not taken into account in FWM signals. The FWM spectra are calculated by the Fourier transformation of $P_{\rm i}(t)$. In addition, the signal from the propagating component of the LBXP should be taken into account in the calculation of FWM spectra. This signal, which is firstly generated in the near-surface region, is calculated independently of the

above calculation as the fast-decay component. The fast-decay component is expressed simply as a Gaussian spectrum with the full width at half maximum (FWHM) of 1.4 meV, which is measured from the SR-FWM signal at the delay time of 0.0 ps as the inhomogeneous broadening of resonances of the propagating LBXP.

The calculated results are shown in Fig. 2(b), and it is to be noted that the calculated spectra are in good agreement with the experimental data shown in Fig. 2(a). The calculation successfully reproduces the exchange of the dominant peak position between the LP and MP at the delay times observed in the experiment. The period of the spectral change is determined by the energy difference between the LP and MP, i.e., the period of the Rabi oscillation. The contrast of the spectral change depends on the strengths of the exciton-exciton interactions. Here, the ratio $U_1 : U_2$ is the only variable parameter for the fitting, and it is set to $1 : -0.2$ for the calculated results in Fig. 2(b). The other parameters are determined by the following estimation.

From the experimental spectrum at the delay time of 4.4 ps, the coupling constant C and the FWHM of inhomogeneous broadening for the LP and MP are obtained to be 0.8 and 0.9 meV, respectively. To determine the strength of the fast-decay component, the experimental TI-FWM signals are compared with the calculation, as shown in Figs. 3(a) and 3(b). In order to obtain the spectrum only for the LP and MP, including the fast-decay component, the intensity is integrated from 2800.7 to 2805.0 meV for the TI-FWM measurement. The dip at the delay time of 0.8 ps in Fig. 3(a) indicates the shift from the fast-decay component of the propagating LBXP to the LP and MP. The fast-decay component is dominant until the delay time of 0.8 ps, because the LP and MP peaks rise gradually, as shown in Fig. 3(b). The decay times for the fast-decay component and the two peaks are obtained to be 0.7 and 2.4 ps, respectively. The exchange behavior of the dominant peak position explicitly reflects the initial creation process, and it is sensitive to the amplitudes of the LBXP and DX in the initial process, and also to the ratio $U_1 : U_2$. Using the above parameters determined by the experimental results and tuning the variable parameter $U_1 : U_2$, we have accurately reproduced the spectral change.

Finally, we discuss the validity of the variable parameter $U_1 : U_2$. The ratio in the calculation of Fig. 2(b), i.e., $U_1 : U_2 = 1 : -0.2$, is determined by the contrast of the spectral change in the experimental results. For comparison to this ratio, the FWM spectra are calculated with different ratios, as shown in Figs. 4(a) and 4(b), in which the U_1 and U_2 interaction terms are calculated, respectively. The exchange of the dominant peak position is obtained in both interactions; however, the dominant peaks appear on opposite sides at each delay time. As shown in Fig. 2(a), the U_1 interaction dominates the experimentally observed spectra. This strength difference between the two interactions is explained by biexciton formation. For excitation by cocircularly polarized pulses, only biexcitons including both hh and lh excitons are generated; there is no biexciton composed of two hh excitons or two lh excitons as reported in a previous investigation.[11] The hh-lh exciton interaction is used not only for the FWM signals from the exciton-polaritons, but also for biexciton formation. Therefore, the

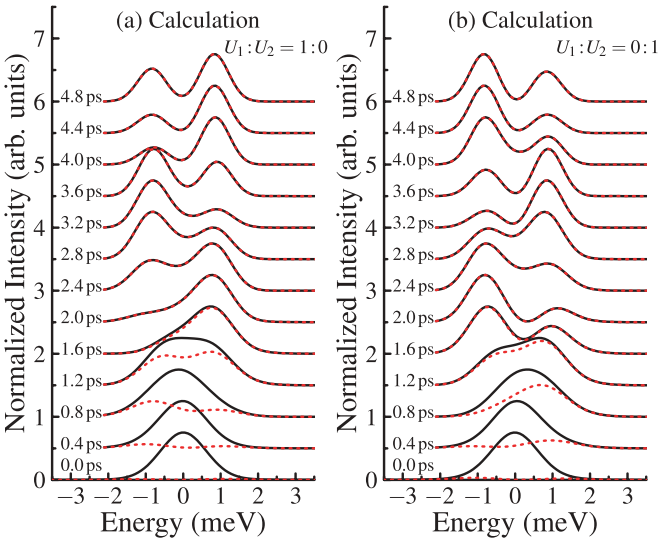

FIG. 4. (Color online) Calculation of spectrally resolved FWM signal for delay times from 0.0 to 4.8 ps in 0.4-ps steps as indicated. (a) $U_1 : U_2 = 1 : 0$ and (b) $U_1 : U_2 = 0 : 1$. The signal indicated by the dotted line is calculated without the fast-decay component. The spectra are normalized for each delay time.

U_2 interaction contributes weakly to the exciton-polariton peaks.

IV. CONCLUSION

We have investigated the coherent dynamics of three-branch exciton-polaritons in a ZnSe epitaxial layer. We have observed a coherent spectral change between the lower and middle polariton branches, which directly reflects the dynamical mixing and nonlinear interactions between the polaritons. From the calculation based on the exciton-photon microscopic model, it has been found that the spectral change is well described by the four-particle correlations between heavy-hole and light-hole excitons and the Rabi oscillation between the polaritons. The quantitative agreement between experimental and theoretical results indicates the observation of the initial creation process of exciton-polaritons.

ACKNOWLEDGMENTS

This work was supported by the Global Center of Excellence Program by MEXT, Japan, through the Nanoscience and Quantum Physics Project of the Tokyo Institute of Technology.

APPENDIX: DISPERSIONS OF A THREE-BRANCH POLARITON

In the ZnSe epitaxial layer with the thickness of 4.7 μm, the valence band is split into the heavy-hole (hh) and light-hole (lh) bands, because of the biaxial tensile strain due to the lattice mismatch and the difference in thermal expansion between the ZnSe layer and the GaAs substrate. Due to the mixing of the photon, hh, and lh excitons, the dispersions of a three-branch polariton are expressed as the eigenvalues of the following

matrix:

$$\begin{pmatrix} E_{\rm ph}(k) & \sqrt{3}g/2 & -g/2 \\ \sqrt{3}g^*/2 & E_{\rm hh}(k)+3\Delta/4 & -\sqrt{3}\Delta/4 \\ -g^*/2 & -\sqrt{3}\Delta/4 & E_{\rm lh}(k)+\Delta/4 \end{pmatrix} \quad \text{(A1)}$$

with

$$E_{\rm ph}(k) = \frac{\hbar c}{n}k, \quad \text{(A2)}$$

$$E_{\rm hh}(k) = E_0 + \frac{\hbar^2}{2M_{\rm h}}k^2 + S_{\rm hh}, \quad \text{(A3)}$$

$$E_{\rm lh}(k) = E_0 + \frac{\hbar^2}{2M_{\rm l}}k^2 + S_{\rm lh}, \quad \text{(A4)}$$

where the excitation of right circularly polarized light is taken into account for the exciton transitions. The dispersions of the photon, hh, and lh excitons are expressed as $E_{\rm ph}(k)$, $E_{\rm hh}(k)$, and $E_{\rm lh}(k)$ with a wave vector k, respectively. In these equations, c is the light velocity; n is the refractive index of ZnSe; E_0 is the exciton energy at $k = 0$ in the unstrained state; $M_{\rm h}$ and $M_{\rm l}$ are the effective masses of hh and lh excitons, respectively; $S_{\rm hh}$ and $S_{\rm lh}$ are the energy shifts due to the strain for hh and lh excitons. The transition matrix elements of hh and lh excitons are expressed as $\sqrt{3}g/2$ and $-g/2$, respectively. The exchange interaction between electron and hole, Δ, is not sufficiently strong to change the dispersions overall. It changes only near the degenerate point between the hh and lh excitons around the wave vector of 18×10^5 cm^{-1}. These constants have been reported to be $n = 2.85$, $|g| = 55.5$ meV, $\Delta = 0.45$ meV, $M_{\rm h} = 1.11m_0$, and $M_{\rm l} = 0.38m_0$, where m_0 is the free-electron mass, in previous investigations.[17,18] The light-matter coupling strength $|g|$ is calculated from the longitudinal-transverse splitting of excitons in ZnSe.

For the splitting due to the biaxial tensile strain, the strain tensors ε_{ij} are given by

$$\varepsilon_{xx} = \varepsilon_{yy} = \varepsilon, \quad \text{(A5)}$$

$$\varepsilon_{zz} = -\frac{2C_{12}}{C_{11}}\varepsilon, \quad \text{(A6)}$$

$$\varepsilon_{xy} = \varepsilon_{yz} = \varepsilon_{zx} = 0, \quad \text{(A7)}$$

where z is defined as the direction parallel to the [001] axis. C_{11} and C_{12} are the elastic stiffness constants, and ε is the magnitude of biaxial strain, which is defined to be positive for tensile strain. The energy shifts due to the strain are expressed as[15,16,18]

$$S_{\rm hh} = 2a\frac{C_{11}-C_{12}}{C_{11}}\varepsilon - b\frac{C_{11}+2C_{12}}{C_{11}}\varepsilon, \quad \text{(A8)}$$

$$S_{\rm lh} = 2a\frac{C_{11}-C_{12}}{C_{11}}\varepsilon + b\frac{C_{11}+2C_{12}}{C_{11}}\varepsilon, \quad \text{(A9)}$$

where $a = a_{\rm c} - a_{\rm v}$ with the hydrostatic deformation potential $a_{\rm c}$ ($a_{\rm v}$) for the conduction (valence) band, and b is the shear deformation potential. The polariton dispersions in Fig. 1(a) are calculated by using the following parameters: $E_{\rm hh}(0) = 2803.5$ meV and $E_{\rm hh}(0) - E_{\rm lh}(0) = 2.1$ meV, which corresponds well to the splitting reported in previous investigations.[15,16,18]

In order to analyze the polariton features for three branches, we have calculated the following components. The bright exciton (BX) with $J = 1$ and $J_z = \pm 1$ and dark exciton (DX) with $J = 2$ and $J_z = \pm 1$ are expressed as linear combinations of hh and lh excitons. The wave functions of the BX ($|{\rm BX}\rangle$) and DX ($|{\rm DX}\rangle$) are given by

$$|{\rm BX}\rangle = \frac{\sqrt{3}}{2}|{\rm hh}\rangle - \frac{1}{2}|{\rm lh}\rangle, \quad \text{(A10)}$$

$$|{\rm DX}\rangle = \frac{1}{2}|{\rm hh}\rangle + \frac{\sqrt{3}}{2}|{\rm lh}\rangle, \quad \text{(A11)}$$

where $|{\rm hh}\rangle$ and $|{\rm lh}\rangle$ are the wave functions of hh and lh excitons, respectively. The eigenenergies of the BX and DX are expressed as

$$E_{\rm BX}(k) = \frac{1}{4}(3E_{\rm hh}(k) + E_{\rm lh}(k)) + \Delta, \quad \text{(A12)}$$

$$E_{\rm DX}(k) = \frac{1}{4}(E_{\rm hh}(k) + 3E_{\rm lh}(k)). \quad \text{(A13)}$$

The DX is optically forbidden, but the optically allowed BX is coupled with a photon, which generates upper and lower bright exciton-polaritons (UBXP and LBXP). The eigenenergies of the UBXP and LBXP are expressed as

$$E_{\rm UBXP}(k) = \frac{1}{2}E_1(k) + \frac{1}{2}\sqrt{E_2(k)^2 + 4|g|^2}, \quad \text{(A14)}$$

$$E_{\rm LBXP}(k) = \frac{1}{2}E_1(k) - \frac{1}{2}\sqrt{E_2(k)^2 + 4|g|^2}, \quad \text{(A15)}$$

where $E_1(k) = E_{\rm ph}(k) + E_{\rm BX}(k)$ and $E_2(k) = E_{\rm ph}(k) - E_{\rm BX}(k)$. The dispersions of $E_{\rm UBXP}(k)$, $E_{\rm LBXP}(k)$, and $E_{\rm DX}(k)$ are shown in Fig. 1(a) with the dispersions of a three-branch polariton.

[1] D. Fröhlich, A. Kulik, B. Uebbing, A. Mysyrowicz, V. Langer, H. Stolz, and W. von der Osten, Phys. Rev. Lett. **67**, 2343 (1991).

[2] H. Giessen, A. Knorr, S. Haas, S. W. Koch, S. Linden, J. Kuhl, M. Hetterich, M. Grün, and C. Klingshirn, Phys. Rev. Lett. **81**, 4260 (1998).

[3] N. C. Nielsen, S. Linden, J. Kuhl, J. Förstner, A. Knorr, S. W. Koch, and H. Giessen, Phys. Rev. B **64**, 245202 (2001).

[4] M. Wegener, D. S. Chemla, S. Schmitt-Rink, and W. Schäfer, Phys. Rev. A **42**, 5675 (1990).

[5] H. Wang, K. Ferrio, D. G. Steel, Y. Z. Hu, R. Binder, and S. W. Koch, Phys. Rev. Lett. **71**, 1261 (1993).

[6] K. Bott, O. Heller, D. Bennhardt, S. T. Cundiff, P. Thomas, E. J. Mayer, G. O. Smith, R. Eccleston, J. Kuhl, and K. Ploog, Phys. Rev. B **48**, 17418 (1993).

[7] E. J. Mayer, G. O. Smith, V. Heuckeroth, J. Kuhl, K. Bott, A. Schulze, T. Meier, D. Bennhardt, S. W. Koch, P. Thomas, R. Hey, and K. Ploog, Phys. Rev. B **50**, 14730 (1994).

[8] Th. Östreich, K. Schönhammer, and L. J. Sham, Phys. Rev. B **58**, 12920 (1998).

[9] J. M. Shacklette and S. T. Cundiff, Phys. Rev. B **66**, 045309 (2002).

[10] H. Haug and S. W. Koch, *Quantum Theory of the Optical and Electronic Properties of Semiconductors* (World Scientific, Singapore, 2009), 5th ed.

[11]H. P. Wagner, W. Langbein, and J. M. Hvam, Phys. Rev. B **59**, 4584 (1999).
[12]H. P. Wagner, A. Schätz, W. Langbein, J. M. Hvam, and A. L. Smirl, Phys. Rev. B **60**, 4454 (1999).
[13]V. M. Axt, B. Haase, and U. Neukirch, Phys. Rev. Lett. **86**, 4620 (2001).
[14]V. M. Axt, T. Kuhn, B. Haase, U. Neukirch, and J. Gutowski, Phys. Rev. Lett. **93**, 127402 (2004).
[15]T. Yao, Y. Okada, S. Matsui, K. Ishida, and I. Fujimoto, J. Cryst. Growth **81**, 518 (1987).
[16]F. Minami, Y. Kato, K. Yoshida, K. Inoue, and K. Era, Appl. Phys. Lett. **59**, 712 (1991).
[17]B. Sermage and G. Fishman, Phys. Rev. B **23**, 5107 (1981).
[18]S. Permogorov, H. Stolz, H. Vogelsang, Th. Weber, W. von der Osten, P. Kuznetov, A. N. Pechonov, and A. S. Nasibov, Solid State Commun. **88**, 705 (1993).
[19]G. Fishman, Solid State Commun. **27**, 1097 (1978).
[20]J. Erland and I. Balslev, Phys. Rev. A **48**, R1765 (1993).
[21]J. Erland, K.-H. Pantke, V. Mizeikis, V. G. Lyssenko, and J. M. Hvam, Phys. Rev. B **50**, 15047 (1994).
[22]M. Kuwata-Gonokami, S. Inouye, H. Suzuura, M. Shirane, R. Shimano, T. Someya, and H. Sakaki, Phys. Rev. Lett. **79**, 1341 (1997).
[23]T. Aoki, G. Mohs, M. Kuwata-Gonokami, and A. A. Yamaguchi, Phys. Rev. Lett. **82**, 3108 (1999).
[24]T. Yajima and Y. Taira, J. Phys. Soc. Jpn. **47**, 1620 (1979).